Hydrothermal synthesis of titanate nanotubes followed by electrodeposition process

Gil-Sung Kim, Young-Soon Kim, Hyung-Kee Seo and Hyung-Shik Shin[†]

Thin Film Technology Laboratory, School of Chemical Engineering, Chonbuk National University, Jeonju 561-756, Korea

Abstract−Titanate nanotubes were synthesized by hydrothermal process using commercial titania nanoparticles. The experiments were carried out as a function of reaction time, temperature, and NaOH concentration. Furthermore, the titanate nanotube film was fabricated on the Si substrate using electrodeposition method with 60 V and at room temperature. The specimens were investigated by using various techniques such as field-emission scanning electron microscopy (FESEM), transmission electron microscopy (TEM), X-ray diffraction (XRD), Raman Spectroscopy, and X-ray photoelectron spectroscopy (XPS). The formation of sodium titanate nanotubes was affected strongly by the variation in all parameters. The best conditions for the titanate nanotubes were found to be a reaction temperature of 150 °C, 10 M NaOH concentration, and reaction time of 48 hr. Under the best conditions, the resulting titanate nanotubes did not contain any remains of starting material, namely P25 nanoparticles, and also the resulting nanotubes had very smooth morphology with a diameter of ~10 nm and length extending up to several micrometers without presence of any bundle-like structures. The washing of sodium titanate nanotubes with HCl solution leads to conversion into protonic titanate nanotubes via ion exchange reaction. The subsequent sintering of the titanate nanotubes renders dehydration of inter-layered OH groups, thereby leading to precipitation of anatase phase. The tubular structure also gets destroyed during phase change, beyond 375 °C. The electrodeposited titanate film with 60 V for 10 min at room temperature was dense and uniform. In this work, we suggest that electrochemical deposition method of titanate nanotubes film can be used for its applications.

Key words: Electrodeposition, Titanium Dioxide, Solar Cell, Titanate Nanotubes, Hydrothermal Process

INTRODUCTION

Nanosized materials have received increasing attention in various fields by virtue of their special chemical and physical properties. Much work has recently been done on the synthesis and applications of nanosized metal oxides, such as TiO_2, ZnO, SiO_2, etc because of their peculiar catalytic behaviors, nonlinear optical properties, and unusual luminescence responses [Kim et al., 2005a, b; Lee et al., 2003; Nam and Han, 2003; Oh et al., 2005]. Among these materials, nanosized titanium dioxide has attracted great interest because it exhibits many modified electronic and optical properties, and hence resulting extensive applicability in fields including photo-catalysis [Fujishima and Honda, 1972; Nam and Han, 2003; Oh et al., 2005], environment purification [Na et al., 2005], dye-sensitized solar cells [O'Regan and Gratzel, 1991; Chevaleevski and Larina, 2001], gas and humidity sensors [Kim and Lee, 2001]. The performance in a given application is, however, strongly influenced by the crystalline structure, the morphology and also the size of particles. Therefore, one-dimensional (1D) nanostructured TiO_2 materials such as nanotubes, nanowires, nanoribbons, and nanorods have attracted extensive attention due to their great potential for use in these applications.

A considerable amount of studies on various synthesis methods of the 1D nanostructured TiO_2 materials have been carried out. Hoyer synthesized TiO_2 nanotubes with diameters of 70-100 nm using sol-gel method. Imai et al. prepared anatase TiO_2 nanotubes in porous

alumina membranes. Also, Seo et al. manufactured tubular TiO_2 material by digestion of the crystalline (anatase phase) powder using $TiCl_4$. Whereas, rutile powder was used as a starting material for preparing TiO_2 nanotubes with diameter of ~8 nm and length of ~100 nm in 10 M NaOH solutions using hydrothermal method [Kasuga et al., 1998]. Recently, it was also reported that TiO_2 nanofibers and/or nanotubes could be synthesized by use of various types of templates, such as porous alumina, organic eggshell membrane, and surfactant assemblies. The TiO_2 nanofibers and/or nanotubes obtained by use of templates have larger diameter and thicker walls composed of nanoparticles. The hydrothermal methods, however, were found to be better and more convenient for preparing TiO_2 nanotubes. In this method, anatase or anatase-rutile TiO_2 nanoparticles were treated with an aqueous solution of 10 M NaOH at 150 °C, to convert TiO_2 particles into nanotubes. The formation mechanism of TiO_2 nanotubes has been in controversy. In this context, Du et al. reported that TiO_2 nanotubes are formed before the washing treatment because the nanotubes do not consist of pure framework of TiO_2 but are of protonic titanate nature. Chen et al. insisted that nanotubes could be constructed in the form of hydrogen titanate phase because sodium titanate nanotube structure changes to hydrogen titanate nanotubes during washing and HCl treatment via ion exchange of Na^+ by H^+. To date, the electrochemical deposition of metal oxides can be expected to be precisely controlling the film thickness and morphology and obtaining lower cost [Lee et al., 2005; Godbole et al., 2005]. Especially, electrochemical deposition of titanate nanotubes will become more important in the future.

In the present studies, commercial titania powder (P25, Degussa, Germany) was used as a starting material. It was added to NaOH

[†]To whom correspondence should be addressed.
E-mail: hsshin@chonbuk.ac.kr

solutions of various concentrations so that sodium titanate nanotubes could be obtained by heating it in the temperature range of 110 °C to 180 °C. In the process, the influence of reaction time, temperature, and NaOH concentration on the crystalline transformation and morphology was estimated. The morphology and phase transformation of partially ion-exchanged titanate nanotubes by heat treatment at the temperature range of 375 °C to 450 °C in atmosphere was also investigated. The characteristic states of the electrodeposited films were also discussed.

EXPERIMENTAL

Commercial titania powder (P25, Degussa, Germany) was used without any purification treatment as a starting material to prepare sodium titanate nanotubes by hydrothermal method. Two grams of powder was added to 75 ml of 3-10 M NaOH solutions in a Teflon vessel under stirring and the so-obtained mixture was taken into a Teflon-lined autoclave of 100 ml. Finally, the autoclave was sealed into a stainless tank and placed in the oven at the temperature of 110 °C to 180 °C by changing reaction time for synthesis of sodium titanate nanotubes. After reaction, the precipitates of sodium titanate nanotubes were filtered, repeatedly washed with distilled water until the pH value became neutral to prevent agglomeration of precipitates. The so-obtained precipitates were dried at 60 °C for 12 hr
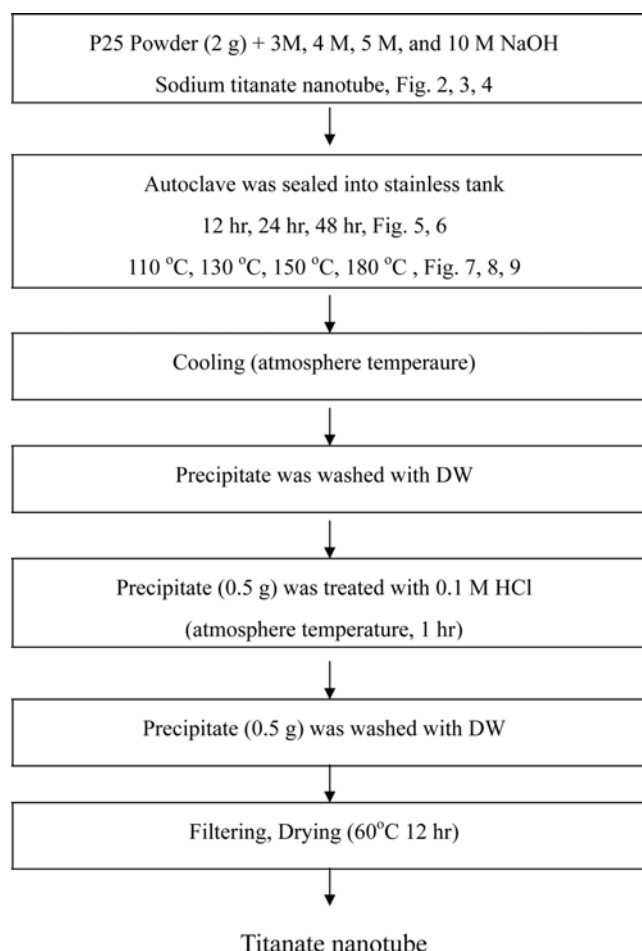
or more to obtain sodium titanate nanotubes. The detailed synthesis process is presented in Fig. 1. Finally, titanate nanotubes were filtered out and washed thoroughly with HCl solution and then distilled water so that the pH value reached 7.

The coating of titanate nanotubes on <100> silicon was carried out by using electrodeposition method. Titania nanotubes were mixed in distilled water and methanol was used as an electrolyte. In these experiments, silicon (size ~15 mm×10 mm) was used as an anode and silver (Ag) was used as a counter (cathode) electrode. A constant voltage of 60 V was applied and time of deposition was for 10 min.

The crystalline structures of the sodium titanate nanotubes were analyzed with X-ray diffractometer (Rikagu D/Max P/N: 3 kW/40 kV, 30 mA) with CuKα (λ=1.54056 Å). The morphology was studied with a field-emission scanning electron microscope (Hitach, S-4700), while elemental identification was carried out by energy dispersive analysis of X-rays. Transmission electron microscopy (JEOL, JEM-2010) has also been used for topological studies, while selected area electron diffraction patterns (SAED patterns in TEM) were recorded to bring out structural information. The surface chemical bonding was analyzed by X-ray photoelectron spectroscopy (XPS, Model - Kratos Amicus). Raman Spectroscopy (Renishaw, Micro Raman) with excitation source Ar$^+$ laser (λ=514.5 nm) was also utilized for understanding bonding configuration (and hence

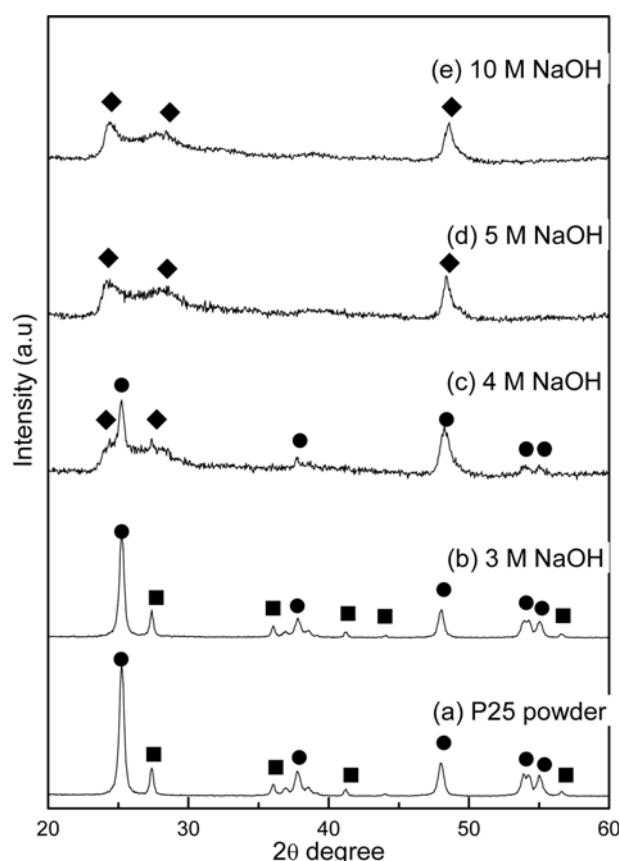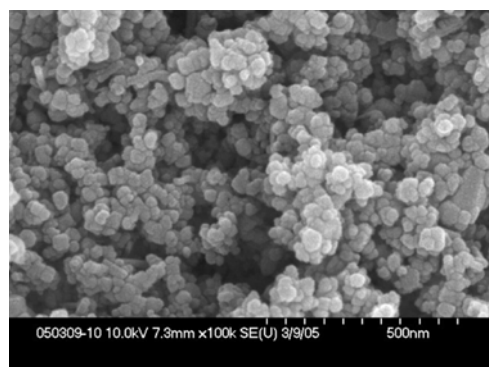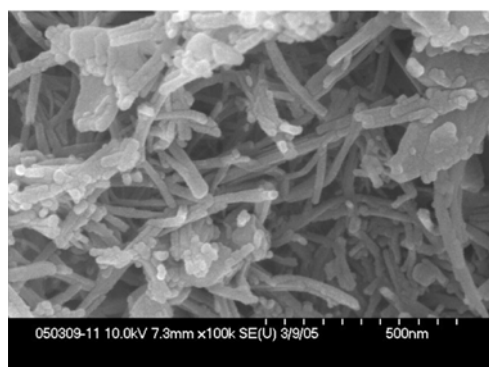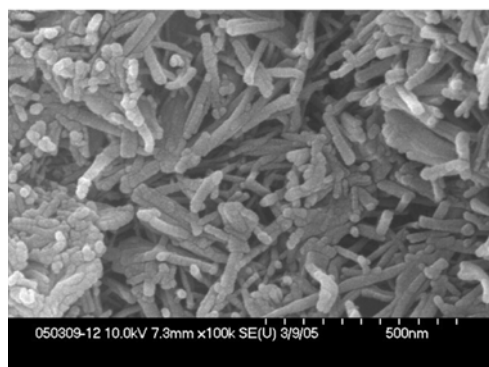**Fig. 1. The synthesis steps of titanate nanotube.**

Fig. 2. XRD patterns of P25 powder and sodium titanate nanotubes prepared in various concentrations of NaOH solutions at 150 °C hydrothermal treatment temperature for 48 hr: (a) P25 powder, (b) 3 M NaOH, (c) 4 M NaOH, (d) 5 M NaOH, and (e) 10 M NaOH (● anatase, ■ rutile, and ◆ sodium titanate nanotubes).
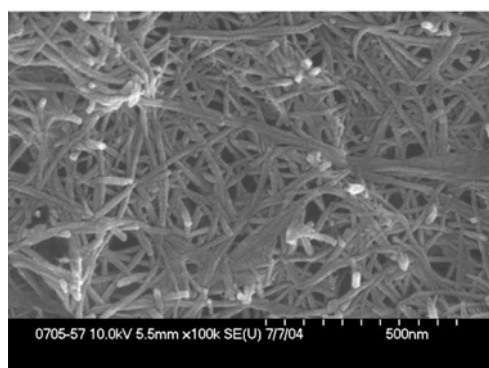
(a)

(b)

(c)

(d)

Fig. 3. High resolution SEM micrographs showing formation of the fibrous particles after reaction of P25 powder with various concentration of NaOH solution at 150 °C for 48 hr (hydrothermal treatment): (a) 3 M NaOH, (b) 4 M NaOH, (c) 5 M NaOH, and (d) 10 M NaOH.

structural information) via optical scattering.

RESULTS AND DISCUSSION

1. Studies on Sodium Titanate Nanotubes

1-1. Effect of NaOH Concentration

Fig. 2 shows the XRD patterns of P25 powder and sodium titanate nanotubes prepared at 150 °C for 48 hr in various concentrations of NaOH solutions. As identified in the figure, the peak positions and relative intensities in the diffraction pattern corresponding to P25 powder (Fig. 2(a)) are almost identical to those of the particles obtained from 3 M NaOH solution (Fig. 2(b)). The pattern of the particles, however, obtained from 4.0 M NaOH solution indicates that some characteristic peaks of P25 powder disappeared and new peaks corresponding to sodium titanate nanotubes appeared. Also, as the concentration of NaOH solution increases, the peak intensities of P25 powder decrease and those of sodium titanate nanotubes increase and finally at 10 M NaOH only the peaks at $2\theta=24°$, 28° and 48°, corresponding to sodium titanate nanotubes, are observed. It is meaning that P25 powder completely transformed to sodium titanate nanotubes. Previously, we reported that the less intense and broad peaks are due to the titanate nanotubes containing sodium ($Na_2Ti_3O_7$), which is in good agreement with the reported titanate nanotubes work [Godbole et al., 2005; Kim et al., 2006].

Fig. 3 shows high resolution SEM micrographs of fibrous materials, prepared by hydrothermal method at 150 °C for 48 hr in the
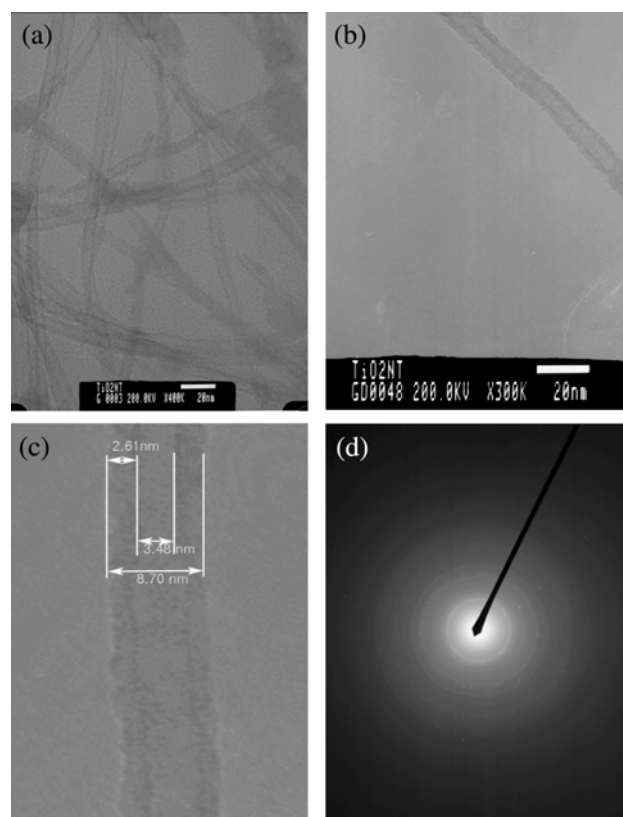

Fig. 4. (a) TEM images on the center, (b) on the edge, (c) high-resolution TEM (HRTEM), and (d) the selected area electron diffraction (SAED) pattern of sodium titanate nanotube obtained from the 10 M of NaOH solution.

various concentration of NaOH solution. Fig. 3(a) shows the image of the particles obtained from 3 M NaOH solution. Many small particles with spherical shape exist in a state of being agglomerated and downy fine particles form the surfaces of the agglomerates, whereas particles with fibrous shape are not observed in this reaction condition. However, as shown in the Fig. 3(b)-(d), it can be seen that particles with fibrous shape are formed in and over 4 M NaOH, and the aspect ratio of the particle increases with increase of NaOH concentration, indicating that the particles grow in the preferred direction of length. The typical diameter and length of obtained fibrous materials is 10-30 nm and 300-500 nm at 5 M and 8-12 nm and ~ several hundred nm at 10 M NaOH, respectively. Here, considering that the original shape of P25 particle is spherical, it is presumed that the thin layers as in Fig. 3(b) might be an intermediate stage of conversion of spheres into fibrous structures with increase of NaOH concentration. It is, therefore, concluded that NaOH concentration is one of the important factors in determining the overall morphological aspects ratio of the fibrous materials.

Fig. 4 shows transmission electron microscopy (TEM) photographs and selected area electron diffraction (SAED) patterns of fibrous materials synthesized at 150 °C for 48 hr in the 10 M NaOH solution. As shown in the figure, typical outer diameter of the obtained nanotubes is ~9 nm and inner diameter ~3.5 nm, indicating the wall thickness of ~2.5 nm since the fibrous particles is tubular

shape. Fig. 4(d) is an SAED pattern taken from an area containing a large amount of sodium titanate nanotube of Fig. 4(a). It is found that the SAED patterns are different from those of TiO_2 due to structural changes from TiO_2 to sodium titanate nanotubes. This result indicates that the shell of tubular structure consists of a quasi-two-dimensional lattice.

1-2. Effect of Reaction Time

Fig. 5 shows the XRD patterns of P25 powder and sodium titanate nanotubes synthesized by use of 10 M NaOH solution at 150 °C

Fig. 6. High resolution SEM micrographs of sodium titanate nanotubes synthesized at 150 °C hydrothermal treatment temperature in the 10 M NaOH solution: (a) for 12 hr, (b) for 24 hr, and (c) for 48 hr.
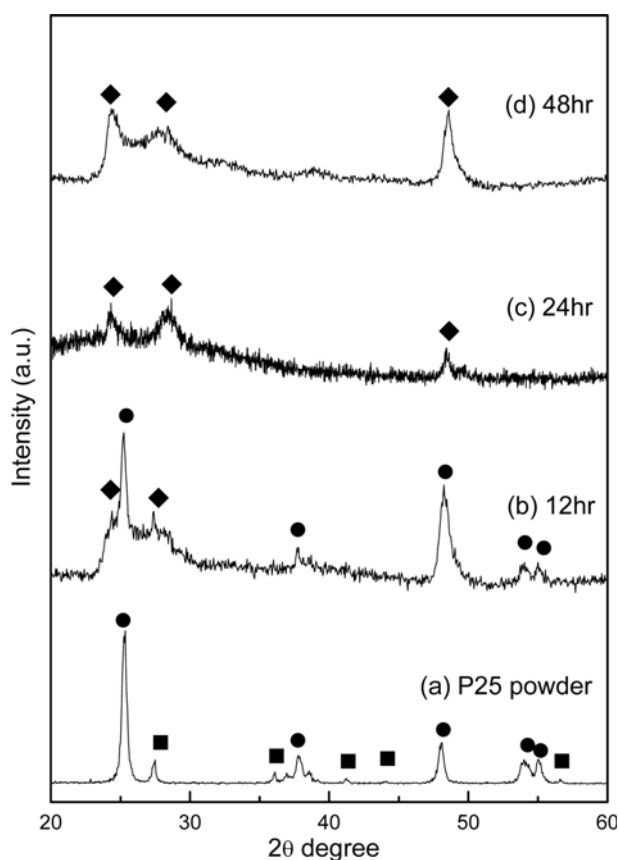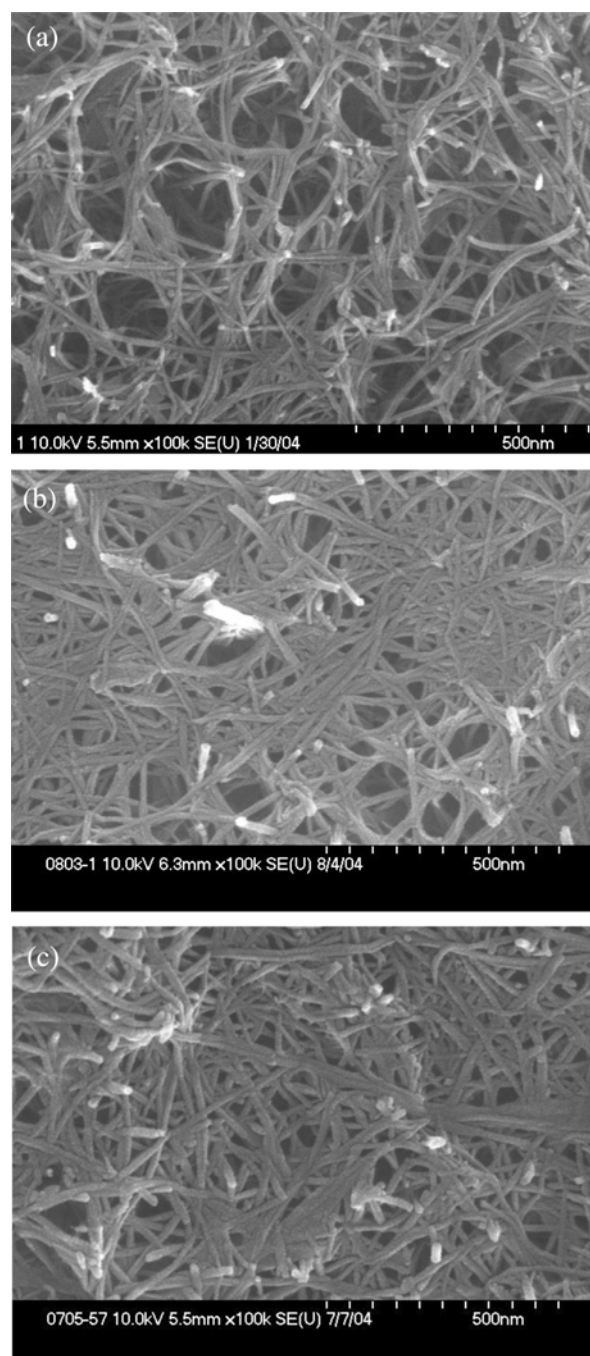

Fig. 5. XRD patterns of (a) P25 powder and sodium titanate nanotubes synthesized at 150 °C hydrothermal treatment temperature in the 10 M NaOH solution: (b) for 12 hr, (c) for 24 hr, and (d) for 48 hr (● anatase, ■ rutile, and ◆ sodium titanate nanotube).

while changing reaction time. As shown in the figure, all the XRD peaks of P25 powder are assigned to anatase and rutile phases whereas the peaks of the particles obtained after 12 hr showed a changed results, identified that the peaks characteristic of rutile (■) in P25 powder disappeared and new peaks corresponding to sodium titanate nanotubes (◆) appeared. After 24 hr, only the sodium titanate nanotube peaks are observed, indicating that P25 particles completely transformed to sodium titanate nanotubes. Also, as the reaction time increases, the peak intensities for sodium titanate nanotubes increase, indicating better crystallinity of nanotube structures. Consequently, it can be said that at least 24 hr of reaction time is required for complete transformation of P25 particles to sodium titanate nanotubes.

Fig. 6 shows high resolution SEM micrographs of sodium titanate nanotubes obtained at 150 °C with different reaction time. As shown in the figure, although the nanotubes obtained at 12 hr exhibit uneven size distribution in diameter and length, the uniformity of nanotubes increases with increase of reaction time, indicating that reaction time plays an important role in imparting specific morphology to the nanostructures.

1-3. Effect of Reaction Temperature

Fig. 7 shows the XRD patterns of P25 powder and sodium titanate nanotubes synthesized in 10 M NaOH solution at various reaction temperatures for 24 hr. As shown in the figure, the X-ray dif-
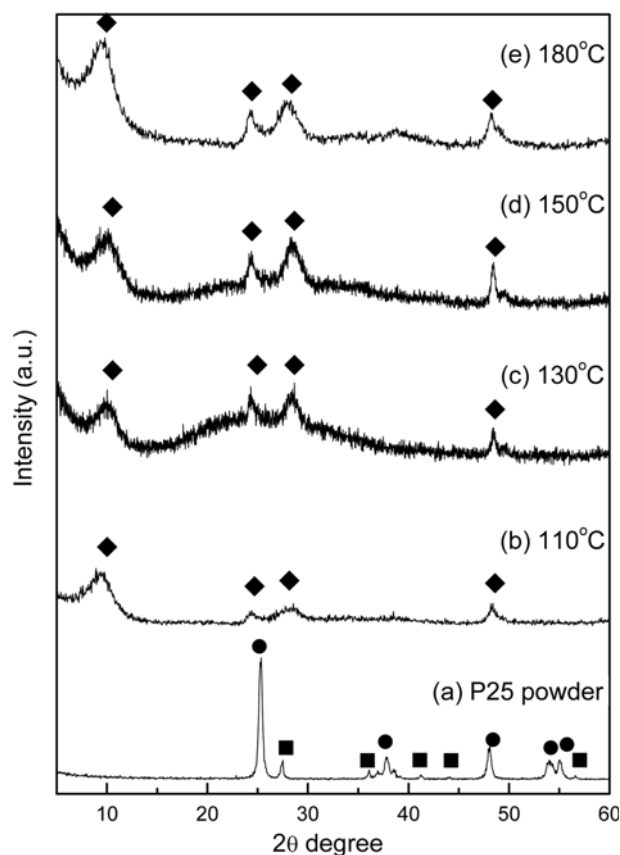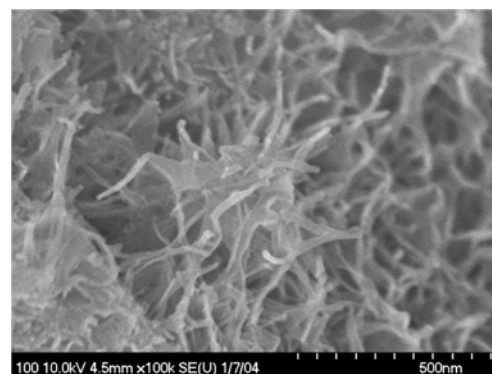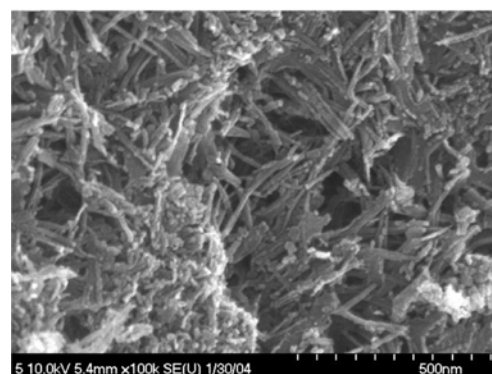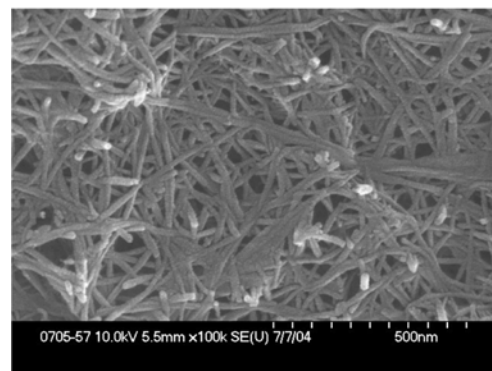

Fig. 7. XRD patterns of (a) P25 powder and sodium titanate nanotubes synthesized at 10 M NaOH solution for 24 hr at: (b) 110 °C, (c) 130 °C, (d) 150 °C, and (e) 180 °C hydrothermal treatment temperature (● anatase, ■ rutile, and ◆ sodium titanate nanotube).
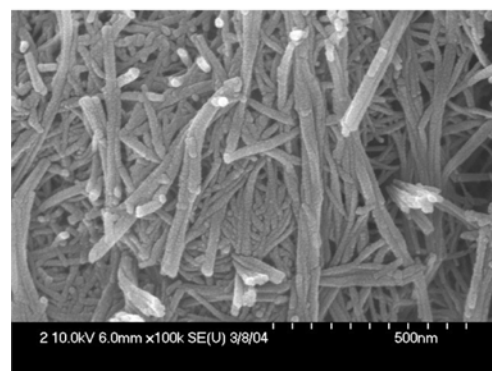

Fig. 8. High resolution SEM micrographs of sodium titanate nanotubes synthesized at 10 M NaOH solution for 24 hr at: (b) 110 °C, (c) 130 °C, (d) 150 °C, and (e) 180 °C hydrothermal treatment temperature.

fraction results reveal that the conversion from P25 powder to sodium titanate nanotube occurs even at a low temperature of 110 °C. At higher temperatures the crystalline quality of tubular structure improves as proved by sharper peaks in the XRD spectrum. Similar results were reported by Seo et al., where they observed an increase in crystallinity with increasing reaction temperature.

Fig. 8 shows high resolution SEM micrographs of sodium titanate nanotubes formed at various temperatures in 10 M NaOH solution for 24 hr. In accordance with the XRD results, these micrographs exhibit formation of tubular structures with improved morphological aspects as the reaction temperature increased. It is also clearly seen that at higher temperature of 180 °C, sodium titanate nanotubes form bundle-like structures due to their self-assembly process. The length of these is found to be up to a few micrometers and the diameters are in the range of 20-50 nm. It is expected that the appearance of higher values of diameters might be due to self-association of smaller diameter nanotubes.

This morphological change is also reflected in the Raman spectroscopy results, as shown in Fig. 9. The Raman spectrum shows broad signals centered around ~280 cm^{-1}, 450 cm^{-1} and 660 cm^{-1}, corresponding Ti-O vibrating modes as in the titania framework

[Yao et al., 2003; Kasuga et al., 1998; Sun et al., 2003, Chen et al., 2002; Zhang et al., 2004]. The intensities of Ti-O vibrating modes increase with the reaction temperature due to the structural changes imparted in going from spherical particle to nanotube form. On the basis of these results it can be inferred that the formation of sodium titanate nanotubes is also affected substantially by reaction temperature.

2. Studies on Titanate Nanotubes

2-1. Preparation of Titanate Nanotubes by Ion Exchange

The partially ion-exchanged titanate nanotubes were prepared by ion exchange reaction of sodium titanate nanotubes with HCl solution. For this purpose, the precipitate (~0.5 g) of sodium titanate nanotubes was stirred in 100 mL of 0.1 M HCl for 1 hr at room temperature and then washed with distilled water several times until the pH value of the effluent reached 7. The precipitate was separated by filtering and then dried under atmosphere at 60 °C for 12 hr. Finally, the dried titanate nanotubes to prepare nanotubular TiO$_2$ (anatase) were sintered at various temperatures for 1 hr in an atmosphere.

2-2. Effect of Heat Treatment on Titanate Nanotubes

In this case, only the effect of post sintering temperature is studied. Fig. 10 shows the XRD patterns of the titanate nanotubes treated for 1 hr at various temperatures up to 450 °C. As indicated by these results, the overall crystallinity of nanotubes is found to enhance
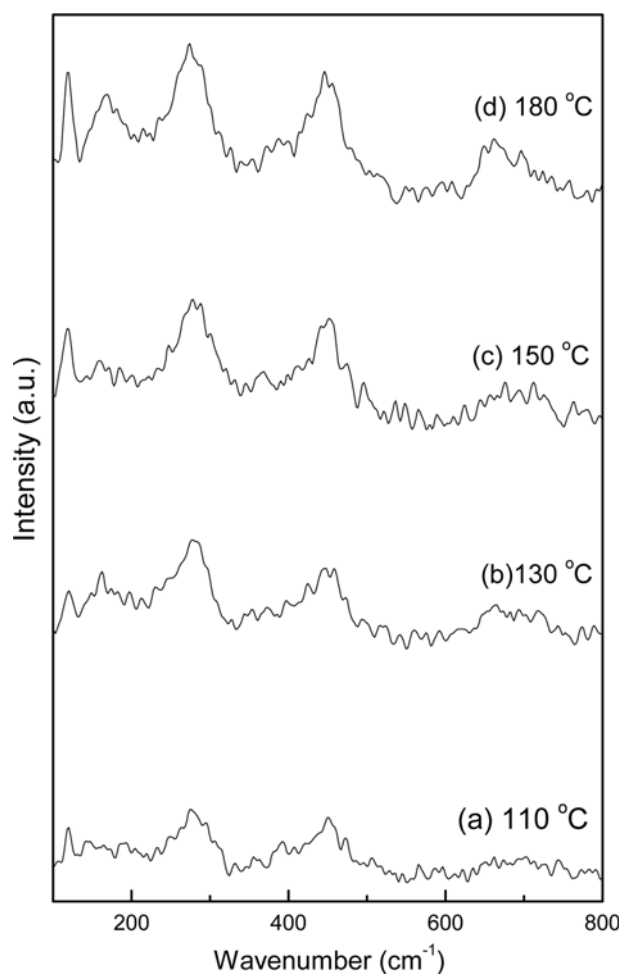

Fig. 9. Raman spectra of sodium titanate nanotubes synthesized at 10 M NaOH solution for 24 hr at: (b) 110 °C, (c) 130 °C, (d) 150 °C, and (e) 180 °C hydrothermal treatment temperature.
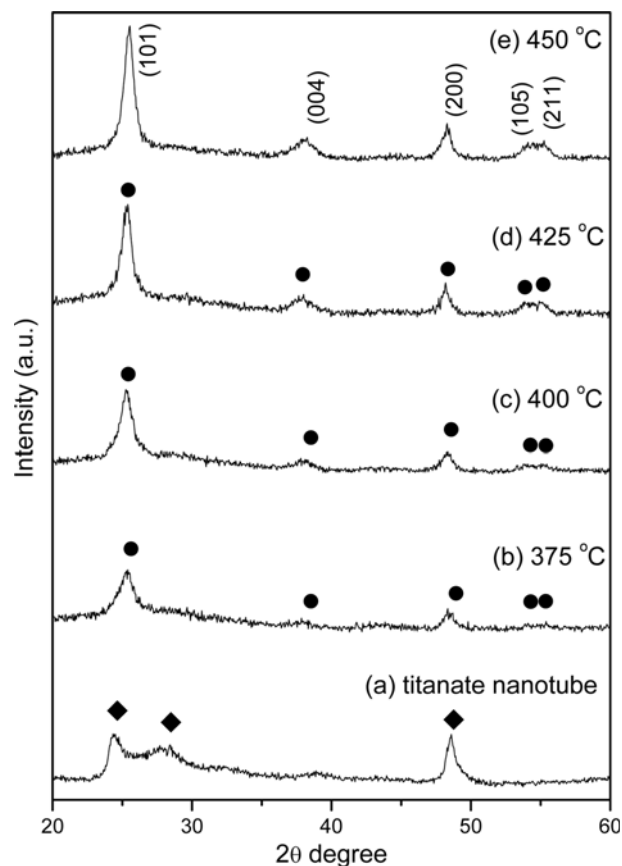

Fig. 10. XRD patterns of the titanate nanotubes sintered for 1 hr at various temperatures: (a) room temperature, (b) at 375 °C, (c) at 400 °C, (d) at 425 °C, and (e) at 450 °C (● anatase and ◆ titanate nanotube).

with sintering temperature. At a higher temperature of 450 °C, the phase of partially ion-exchanged titanate nanotubes disappeared completely and transformed into titania (TiO_2) anatase phase. Diffraction peaks corresponding to the (101), (004), (200), (105), and (211) planes appear in the XRD pattern. These peak positions and their relative intensities are also consistent with the anatase diffraction pattern of P25 powder. No characteristic peaks of the other impurities, such as NaCl, Na_2TiO_3, and rutile phase have been observed. Fig. 11 shows that the TEM micrograph and the select area electron diffraction (SAED) pattern of the titanate nanotubes sintered at 450 °C. The SAED of those nanotubes includes diffraction rings of the (101), (004), (200) and (105) planes of the anatase phase.

All these results reveal that the dehydration of interlayered OH groups induced the change of crystalline structure from titanate nanotubes to pure titania anatase, and also nanotubular structure is destroyed during sintering.

3. Electrodeposited Titanate Nanotubes

The XPS spectra and FESEM image corresponding to electrodeposited titanate film on the Si substrate are shown in Fig. 12. The
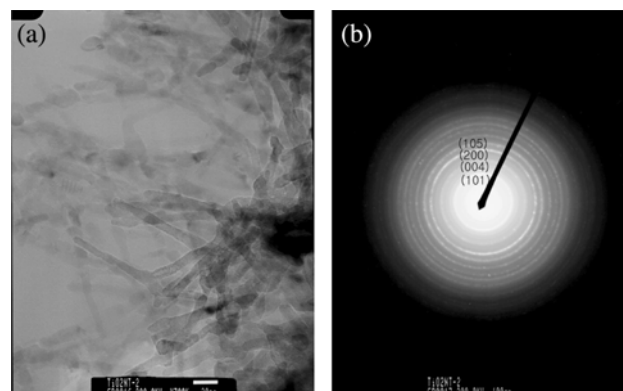

Fig. 11. (a) TEM image and (b) the selected area electron diffraction (SAED) pattern of titanate nanotubes sintered at 450 °C for 1 hr.

peak positions of the sample were referenced to adventitious carbon at 284.75 eV. As can be seen, in a typical wide scan spectra of
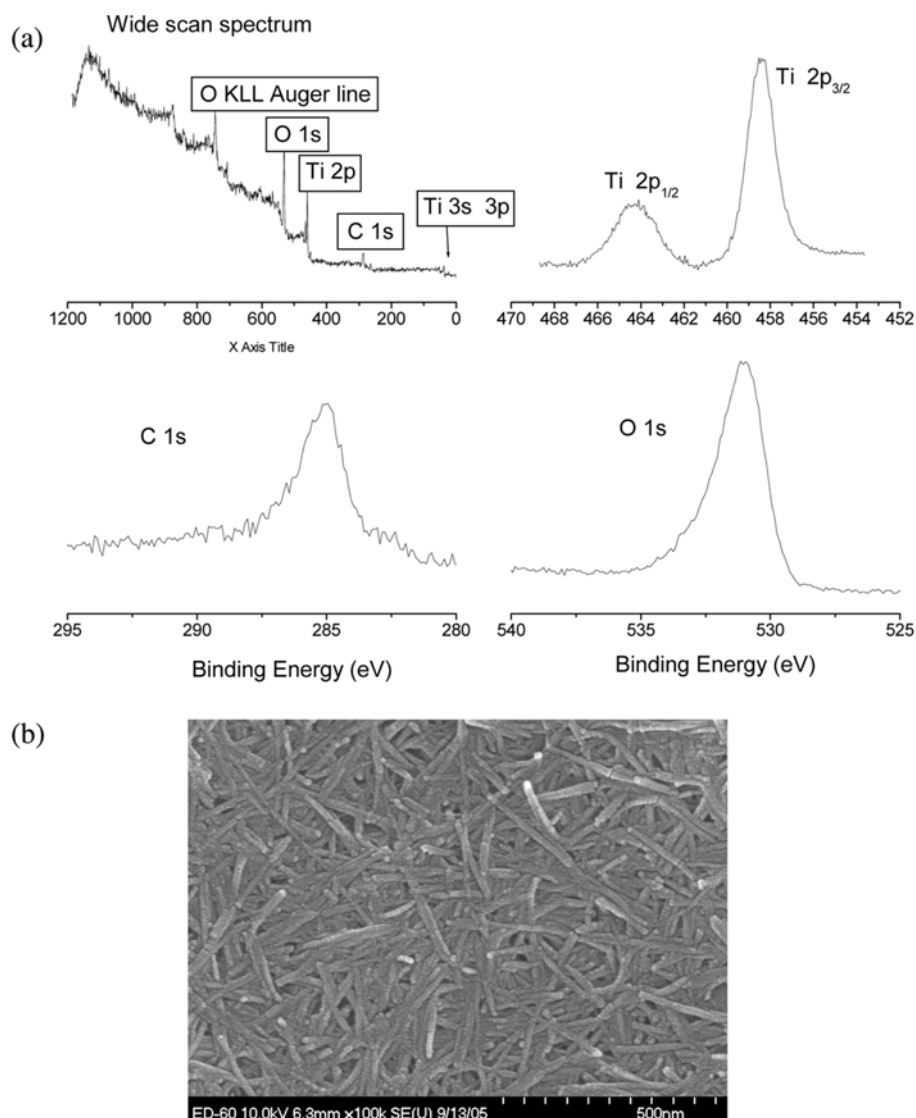

Fig. 12. (a) XPS spectra and (b) top view FESEM image of the electrodeposited titanate film with 60 V at room temperature for 10 min.

Fig. 12(a) all the standard photoelectron lines of Ti in TiO$_2$ are present: Ti 2p, Ti 3s, Ti 3p, O 1s, and adventitious carbon C 1s. The peak, located at around 745 eV, is characterized as the O KLL Auger line. The doublet separation of Ti 2p spectral line is characterized by a binding energy of 458.41 eV (2p$_{3/2}$) with an FWHM of 1.48 eV and 464.28 eV (2p$_{1/2}$) with a separation energy of 5.87 eV. Spectral lines of both the Ti 2p$_{3/2}$ and 2p$_{1/2}$ are very close to the values reported in the literature that Ti 2p$_{3/2}$ has been shown to have a binding energy of 458.8 eV with a separation energy of 5.54 eV [Moulder et al., 1992]. These small discrepancies between measured and reported binding energies are attributed to inadequacies in the calibration of the binding energy scales of individual instruments [Powell, 1995]. The spectral line of O 1s at 531.0 eV indicates titanium oxide (TiO$_x$). The FESEM image of electrodeposited titanate film is shown in Fig. 12(b). The titanate nanotube film was found to be reasonably dense and uniform. We have also tried to change the deposition potentials and to fit the Ti 2p and O 1s spectra by using Shirley type base line with mixed Gaussian (30%) and Lorentzian (70%) profiles. This will be further investigated in a future study.

CONCLUSIONS

Sodium titanate nanotubes have been synthesized by the hydrothermal synthesis of P25 powders. These experiments were carried out by varying reaction parameters such as temperature, concentration of NaOH solution, and reaction time. The experimental results suggest that the formation of sodium titanate nanotubes is affected strongly by the variation in all these parameters. Based on the present research findings, it can be concluded that the best quality sodium titanate nanotubes can be synthesized at a reaction temperature of 150 °C, with 10 M NaOH concentration, and reaction time of 48 hr. The resulting product does not contain any remnants of the starting material, namely P25 nanoparticles, and also the resulting nanotubes have very smooth morphology without the presence of any bundle-like structures. Typically, these nanotubes exhibit ~10 nm diameter and length extending up to several micrometers. The conversion of P25 nanoparticles into nanotubes is believed to occur via initial formation of two dimensional nanolayers, which then undergo the curling mechanism to form a tubular structure.

The washing of sodium titanate nanotubes with distilled water and HCl solution leads to conversion into titanate nanotubes via ion exchange reaction. The subsequent sintering of the titanate nanotubes renders dehydration of interlayered OH groups, thus leading to precipitation of the anatase phase. The tubular structure also gets destroyed during phase change, beyond 375 °C. Subsequently, a dense and uniform titanate film is fabricated on the silicon substrate by using electrodeposition method with 60 V for 120 s and at room temperature. This result indicates that titanate film can be easily fabricated by the electrodeposition method for its application such as dye-sensitized solar cell.

REFERENCES

Chen, Q., Du, G. H., Zhang, S. and Peng, L. M., "The structure of trititanate nanotubes," *Acta Crystallogr. B*, **58**, 587 (2002).

Chen, Q., Zhou, W., Du, G. and Peng, L. M., "Trititanate nanotubes made via a single alkali treatment," *Adv. Mater.*, **14**, 1208 (2002).

Chevaleevski, O. and Larina, L., "New trends in solar photovoltaics: From physics to chemistry," *Korean J. Chem. Eng.*, **18**, 403 (2001).

Du, G. H., Chen, Q., Che, R. C., Yuan, Z. Y. and Peng, L. M., "Preparation and structure analysis of titanium oxide nanotubes," *Appl. Phys. Lett.*, **79**, 3702 (2001).

Fujishima, T. and Honda, K., "Electrochemical photolysis of water at a semiconductor electrode," *Nature*, **238**, 37 (1972).

Godbole, V. P., Kim, G. S., Dar, M. A., Kim, Y. S., Seo, H. K., Khang, G. and Shin, H. S., "Hot filament chemical vapour deposition processing of titanate nanotube coatings," *Nanotechnology*, **16**, 1186 (2005).

Hoyer, P., "Formation of a titanium dioxide nanotube array," *Langmuir*, **12**, 1411 (1996).

Imai, H., Takei, Y., Matsuda, M. and Hirashima, H., "Direct preparation of anatase TiO$_2$ nanotubes in porous alumina membranes," *J. Mater. Chem.*, **9**, 2971 (1999).

Kasuga, T., Hiramatsu, M., Hoson, A., Sekino, T. and Niihara, K., "Formation of titanium oxide nanotube," *Langmuir*, **14**, 3160 (1998).

Kasuga, T., Hiramatsu, M., Hoson, A., Sekino, T. and Niihara, K., "Titania nanotubes prepared by chemical processing," *Adv. Mater.*, **11**(15), 1307 (1999).

Kim, G.-S., Godbole, V. P., Seo, H.-K., Kim, Y.-S. and Shin, H.-S., "Sodium removal from titanate nanotubes in electrodeposition process," *Electrochemistry Communication*, **8**, 471 (2006).

Kim, J. S. and Lee, T. K., "Effect of humidity on the photocatalytic degradation of trichloroethylene in gas phase over TiO$_2$ thin films treated by different conditions," *Korean J. Chem. Eng.*, **18**, 935 (2001).

Kim, J. H., Noh, B. H., Lee, G.-D. and Hong, S.-S., "Hydrothermal synthesis of titanium dioxide using acidic petizing agents and their photocatalytic activity," *Korean J. Chem. Eng.*, **22**, 370 (2005).

Kim, S.-H., Umar, A. and Hahn, Y.-B., "Growth and formation mechanism of sea urchin-like ZnO nanostructures on Si," *Korean J. Chem. Eng.*, **22**, 489 (2005).

Lee, B.-Y., Park, S.-H., Lee, S.-C., Kang, M., Park, C.-H. and Choung, S.-J., "Optical properties of Pt-TiO$_2$ catalyst and photocatalytic activities for benzene decomposition," *Korean J. Chem. Eng.*, **20**, 812 (2003).

Lee, J., Nam, S. C. and Tak, Y., "On the origin of electrodeposition mechanism of ZnO on ITO substrate," *Korean J. Chem. Eng.*, **22**, 161 (2005).

Moulder, J. F., Stickle, W. F., Sobol, P. E. and Bomben, K. D., *Handbook of X-ray photoelectron spectroscopy*, Physical Electronics, Inc. Eden Praire, Minnesota 55344, USA (1992).

Na, Y., Song, S. and Park, Y., "Photocatalytic decolorization of rhodamine B by immobilized TiO$_2$/UV in a fluidized-bed reactor," *Korean J. Chem. Eng.*, **22**, 196 (2005).

Nam, W. S. and Han, G. Y., "A photocatalytic performance of TiO$_2$ photocatalyst prepared by the hydrothermal method," *Korean J. Chem. Eng.*, **20**, 180 (2003).

Oh, C. W., Lee, G.-D., Park, S. S., Ju, C.-S. and Hong, S.-S., "Preparation of nanosized TiO$_2$ particales via ultrasonic irradiation and their

photocatalytic activity on the decomposition of 4-nitrophenol," *Korean J. Chem. Eng.*, **22**, 547 (2005).

O'Regan, B. and Gratzel, M., "A low-cost, high-efficiency solar cell based on dye-sensitized colloidal TiO_2 films," *Nature*, **353**, 737 (1991).

Powell, C. J., "Elemental binding energies for X-ray photoelectron spectroscopy," *Applied Surface Science*, **89**, 141 (1995).

Seo, D. S., Lee, J. M. and Kim, H., "Preparation of nanotube-shaped TiO_2 powder," *J. Cryst. Growth*, **229**, 428 (2001).

Sun, X. and Li, Y., "Synthesis and characterization of ion-exchangeable titanate nanotubes," *Chem. Eur. J.*, **9**, 2229 (2003).

Yao, B. D., Chan, Y. F., Zhang, X. Y., Yang, W. Y. and Wang, N., "Formation mechanism of TiO_2 nanotubes," *Appl. Phys. Lett.*, **82**, 281 (2003).

Zhang, S., Li, W., Jin, Z., Yang, J., Zhang, J., Du, Z. and Zhang, Z., "Study on ESR and inter-related properties of vacuum-dehydrated nanotubed titanic acid," *J. Sol. State Chem.*, **177**, 1365 (2004).